Microsyst Technol (2006) 12: 335–342
DOI 10.1007/s00542-005-0062-2

TECHNICAL PAPER

Mengwei Liu · Jianhua Tong · Liding Wang
Tianhong Cui

Theoretical analysis of the sensing and actuating effects of piezoelectric multimorph cantilevers

Received: 11 March 2005 / Accepted: 1 July 2005 / Published online: 26 November 2005

Abstract The paper presents the modeling of two types of piezoelectric microcantilevers, the two-layer and two-segment piezoelectric cantilevers, in which the two piezoelectric parts perform sensor and actuator functions, respectively. An analytic model is proposed to evaluate the sensing and actuating effects of multiporph microcantilevers formed of several layers or segments of piezoelectric materials. The analytical model is used to analyze the tip deflection of the cantilever and the piezoelectric charge generated on the sensor element as a function of the microcantilever geometry. The cantilevers of sensing and actuation are compared for the different working situations of the two-layer and two-segment cantilevers. The theoretical results can be used to optimize the design of the piezoelectric cantilever structures.

1 Introduction

Microsensors and microactuators are key components of micromanipulation systems such as microrobot, microsurgery, and biological cell manipulation. A smart microsystem integrated with sensors and actuators is desired for manipulating objects and feedbacking force simultaneously. The piezoelectric MEMS devices based on thin-film materials and silicon technology can perform either microsensor or microactuator functions by utilizing the direct or converse piezoelectric effect (Muralt 2000; Li-Peng et al. 2003; Zhang et al. 2003; Kim Hyun et al. 2001; Roger de et al. 1999). Among the piezoelectric devices, the cantilevers are the most frequently investigated structures (Zurn et al. 2001; Luginbuhl et al. 1996; DeVoe and Pisano 1997). As actuation elements, when a voltage is applied to the piezoelectric layer, a tip deflection is obtained. As sensing elements, when a force is applied perpendicularly to the tip of the cantilever, the electric charge can be generated on the top and the bottom electrodes.

Most previous literatures have focused on actuator or sensor applications of the piezoelectric cantilevers. Itoh and Suga (1996), Lee and Itoh (1999) demonstrate the use of self-exited piezoelectric microcantilevers with sensing and actuating capabilities. However, a reference circuit or a PZT pattern with the same size as the free-standing PZT cantilever is required to offset the capacitance charge of the piezoelectric layer of the cantilever. This paper describes the design and structure of two types of piezoelectric microcantilevers based on the different placements of the thin-film piezoelectric materials. They are two-layer and two-segment (namely two segments in one layer) piezoelectric cantilevers. The two piezoelectric parts can be used for the sensing and actuating elements, respectively.

In macroscale applications, several analytical models for the three layered laminate structure with a piezoelectric layer as an actuator, an elastic material layer and a second piezoelectric layer as a sensor have been developed, which include the studies of Costa Branco and Dente (2004) and Du et al. (2003). All of their models ignored the influence of the electrode layers. However, for micromachined devices, the additional layers such as electrodes and electrical isolation layers have to be considered in the models, since their thicknesses are usually on the same order as the piezoelectric film itself. Many models of the multimorph cantilevers have been proposed in recent years. Brissaud et al. (2003) derived an analytical model of a non-symmetric bimorph constituted by a thick piezoelectric film, two electrode layers, and a elastic substrate. In their work,

M. Liu · J. Tong · L. Wang · T. Cui
Microsystem Technology Research Center,
School of Mechanical Engineering,
Dalian University of Technology,
Dalian 116023, People's Republic of China

T. Cui (✉)
Department of Mechanical Engineering, University of Minnesota,
111 Church Street SE, Minneapolis, MN 55455, USA
E-mail: tcui@me.umn.edu
Tel.: +1-612-8125270
Fax: +1-612-6256069

the non-symmetric bimorph is driven by harmonic excitation and used either as an actuator or a sensor. Elka et al. (2004) developed the constitutive equations for the multilayered piezoelectric structures actuated by voltages or charges. In the constitutive equations the electromechanical response is presented as the electromechanical coupling stiffness. A model for piezoelectric multimorph cantilevers extended from the Timoshenko's approach was proposed by DeVoe and Pisano (1997) to investigate the deflection of microactuators. The tip deflection of the mutilayered structure was analyzed by Huang et al. (2004) using a similar model in reference (DeVoe and Pisano 1997). Weinberg (1996) derived a more generic model in which the sensing and actuation performance of the piezoelectric multimorph cantilevers subjected to various mechanical and electrical loadings were investigated. An analytical model for the multimorph beams exited by different internally induced strains, including piezoelectricity, has been reported by Soderkvist (1993). An approximate model was presented by Ephrahim and Nicolae (2004). In this model, all types of induced strain can be incorporated into it.

In the above mentioned models, every layer in the structure has the same material and length. This paper proposes a new model for multilayer cantilever devices in which every layer consists of several segments with different materials. Using this model, the tip deflection and piezoelectric charges of the multimorph cantilevers are analyzed. The actuation and sensing capabilities of the two structures, including the two-layer and two-segment cantilevers, are compared.

2 Structure of the piezoelectric microcantilevers

Figure 1 illustrates the two-layer and two-segment piezoelectric microcantilevers. ZnO or lead zirconate titanate (PZT) formed by sputtering deposition or sol–gel processing can be used as the piezoelectric layers. The silicon substrate layer is fabricated by anisotropic etching. Pt/Ti and Pt layers are used as electrode layers. Two layers of SiO_2 are deposited for electrical isolation. The two types of cantilevers are formed of nine and seven layers, respectively. The former includes two layers of piezoelectric films, and the latter includes one layer of piezoelectric film with two separated top electrodes. Both structures consist of two piezoelectric parts in the series connection, and every piezoelectric part serves as a force sensor or actuator. The top and bottom electrodes of the sensing element are grounded.

3 Model

The model developed next provides the equations of the tip deflection and sensing charges of a piezoelectric multimorph cantilever. The geometry of an m-layer piezoelectric cantilever is shown in Fig. 2. In the figure, the individual layer consists of several segments with different materials, which may be either piezoelectric or purely elastic. The cantilever is separated into n segments in the x-direction. For the model, several assumptions are made as follows:

1. The piezoelectric multimorph structure is in static equilibrium.
2. Every layer spans over the same length, L, and has the same width, ϖ.
3. Because the cantilever beam is relative long, the Euler-Bernoulli model employed in terms of bending and shearing effects are excluded. The beam width and thickness is small compared to its length, and the stress and displacement in the y and z directions are equal to zero.

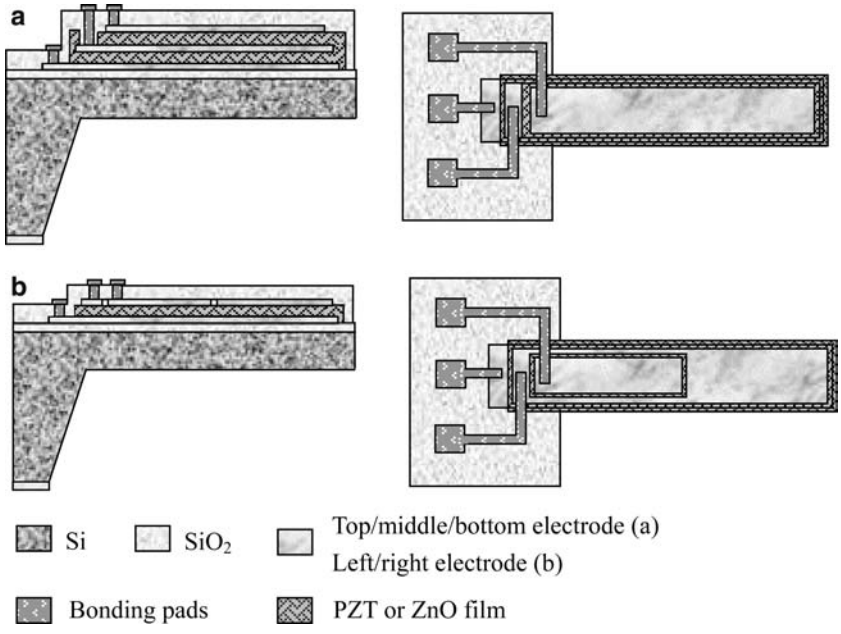

Fig. 1 Schematic diagrams: **a** two-layer cantilever, **b** two-segment cantilever

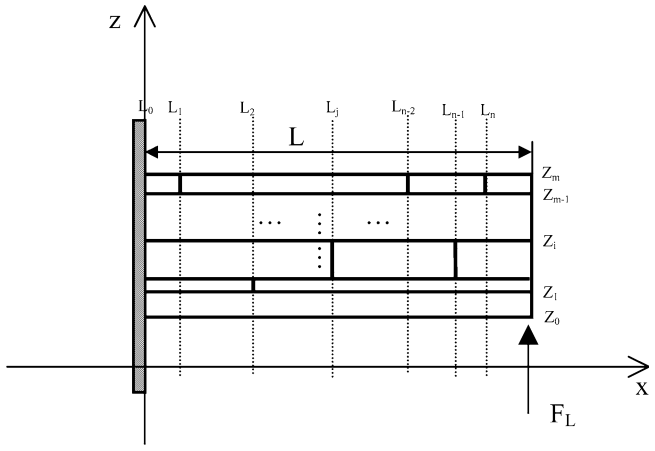

Fig. 2 Geometry of a multimorph composed of m layers and n segments

4. Because the beam width and thickness are very small compared to its length, the displacement in y and z directions can be neglected.
5. Based on assumption (3), the surface charge on the electrodes of the piezoelectric layers are derived from three contributions: (a) transverse piezoelectric effect related to y and z directions, (b) transverse piezoelectric effect related to x and z directions, and (c) longitudinal piezoelectric effect in the z direction. From assumption (4), the two components of (a) and (c) can be neglected.
6. The interfaces between layer i and $i+1$, segment j and $j+1$ are continuous.

For the segment j, the axial forces at any cross section of the m-layer beam sum to zero at equilibrium, which can be written as

$$\sum_{i=1}^{m} P_{ij} = 0. \tag{1}$$

The individual axial force is determined by integrating the normal stress along x-direction over each individual cross section, where the stress variation versus the z coordinate is linear. Using Eq. 1, the total axial force is given by

$$\sum_{i=1}^{m} P_{ij} = \varpi \sum_{i=1}^{m} \int_{z_{i-1}}^{z_i} Y_{ij} S_{ij} \mathrm{d}z = 0, \tag{2}$$

where Y_{ij} and S_{ij} are Young's modulus and the strain along the x-direction of the element of the layer i and segment j, repectively.

According to the interface continuity assumption between adjacent layers, S_{ij} can be written as

$$S_{ij} = (z_{Nj} - z)\frac{\partial^2 \omega_j}{\partial x^2}, \tag{3}$$

where z_{Nj} and ω_j are the position of the neutral axis and the bending displacement along z-axis of the segment j.

Inserting Eq. 3 into 2, perform the integration indicated in 2

$$z_{Nj} = \frac{\sum_i Y_{ij} h_i^2}{\sum_i Y_{ij} h_i} \tag{4}$$

with

$$h_i = z_i - z_{i-1}, \quad h_i^2 = \frac{z_i^2 - z_{i-1}^2}{2}. \tag{5}$$

At any axial position, the internal moments produced by the internal stresses balance the external moments

$$M_{ij} = F_L(L - x) + \varpi \sum_i \int_{z_i} T_{ij} z \mathrm{d}z = 0, \tag{6}$$

where F_L is the force perpendicularly to the tip of the cantilever, and T_{ij} is the stress along the x-direction of the element of the layer i and segment j.

Substituting the constitutive piezoelectric equation

$$T_{ij} = Y_{ij}(S_{ij} - d_{31ij}E_{ij}) \tag{7}$$

and Eq. 3 into Eq. 6, solving the integration over z gives

$$\begin{aligned} &F_L(L-x) \\ &+ \varpi \left[z_{Nj} \frac{\partial^2 \omega_j}{\partial x^2} \sum_i Y_{ij} h_i^2 - \frac{\partial^2 \omega_j}{\partial x^2} \sum_i Y_{ij} h_i^3 - \sum_i Y_{ij} d_{31ij} E_{ij} h_i^2 \right] \\ &= 0 \text{ with } h_i^3 = \frac{z_i^3 - z_{i-1}^3}{3}, \end{aligned} \tag{8}$$

where d_{31ij} is the piezoelectric constant of the piezoelectric material, E_{ij} is the electric field along z-axis inside the piezoelectric material.

Inserting Eq. 5 into Eq. 8, the differential equation for the bending displacement of a multimorph cantilever can be written as

$$\frac{\partial^2 \omega_j}{\partial x^2} = \frac{F_L L + B_j \varpi}{A_j \varpi} - \frac{F_L}{A_j \varpi} x, \tag{9}$$

where A_j and B_j depend on the elastic and geometric parameters of the cantilever beam. B_j also depends on the piezoelectric characteristics and the applied voltage of the piezoelectric layers. A_j and B_j are defined as follows:

$$A_j = \sum_i Y_{ij} h_i^3 - \frac{\left(\sum_i Y_{ij} h_i^2\right)^2}{\sum_i Y_{ij} h_i}, \quad B_j = -\sum_i Y_{ij} d_{31ij} E_{ij} h_i^2. \tag{10}$$

The general solutions to Eq. 9 is

$$\omega_j = \frac{F_L L + B_j \varpi}{2 A_j \varpi} x^2 - \frac{F_L}{6 A_j \varpi} x^3 + C_{1j} x + C_{2j}. \tag{11}$$

The constants C_{1j} and C_{2j} are determined using the boundary conditions of the segment j of the cantilever beam. They can be written as follows:

1. The displacement and slope at the clamped end, located at $x=0$, are equal zero, thus

$$\omega_1(0)=0, \quad \frac{\mathrm{d}\omega_1(0)}{\mathrm{d}z}=0. \tag{12}$$

These equations lead to

$$C_{11}=0, \quad C_{21}=0. \tag{13}$$

When $n=1$, inserting Eqs. 13 into 11, the bending displacement of the cantilever beam can be given by

$$\omega_1=\frac{F_L L+B_1\varpi}{2A_1\varpi}x^2-\frac{F_L}{6A_1\varpi}x^3. \tag{14}$$

2. When $n \geq 2$, the displacement and slope at $x=L_j$ of the segment j are equal to that of the segment $j+1$.

$$\omega_j\big|_{x=L_j}=\omega_{(j+1)}\big|_{x=L_j}, \tag{15}$$

$$\frac{\partial\omega_j}{\partial x}\big|_{x=L_j}=\frac{\partial\omega_{(j+1)}}{\partial x}\big|_{x=L_j}. \tag{16}$$

Solving the Eqs. 15 and 16 leads to

$$\begin{aligned}C_{1(j+1)}=&\left(\frac{F_L L+B_j\varpi}{A_j\varpi}-\frac{F_L L+B_{(j+1)}\varpi}{A_{(j+1)}\varpi}\right)L_j\\&-\left(\frac{F_L}{2A_j\varpi}-\frac{F_L}{2A_{(j+1)}\varpi}\right)L_j^2+C_{1j},\end{aligned} \tag{17}$$

$$\begin{aligned}C_{2(j+1)}=&\left(\frac{F_L L+B_{(j+1)}\varpi}{2A_{(j+1)}\varpi}-\frac{F_L L+B_j\varpi}{2A_j\varpi}\right)L_j^2\\&-\left(\frac{F_L}{3A_{(j+1)}\varpi}-\frac{F_L}{3A_j\varpi}\right)L_j^3+C_{2j}.\end{aligned} \tag{18}$$

By successively applying Eq. 17, the constant C_1 of a particular segment can be expressed in terms of the constant of the previous segment, which, in turn, depends on the constant of the previous segment. In the end, the particular constant is expressed in terms of the constant of the segment 1, thus

$$\begin{aligned}C_{1(j+1)}=&\sum_{j=1}^{j}\left[\left(\frac{F_L L+B_j\varpi}{A_j\varpi}-\frac{F_L L+B_{(j+1)}\varpi}{A_{(j+1)}\varpi}\right)L_j\right.\\&\left.-\left(\frac{F_L}{2A_j\varpi}-\frac{F_L}{2A_{(j+1)}\varpi}\right)L_j^2\right]+C_{11}.\end{aligned} \tag{19}$$

In the same way, Eq. 18 can be written as

$$\begin{aligned}C_{2(j+1)}=&\sum_{j=1}^{j}\left[\left(\frac{F_L L+B_{(j+1)}\varpi}{2A_{(j+1)}\varpi}-\frac{F_L L+B_j\varpi}{2A_j\varpi}\right)L_j^2\right.\\&\left.-\left(\frac{F_L}{3A_{(j+1)}\varpi}-\frac{F_L}{3A_j\varpi}\right)L_j^3\right]+C_{21}.\end{aligned} \tag{20}$$

Inserting Eqs. 13, 19 and 20 into 11, the bending displacement of segment j can be given by

$$\begin{aligned}\omega_j=&\tfrac{F_L L+B_j\varpi}{2A_j\varpi}x^2-\tfrac{F_L}{6A_j\varpi}x^3\\&+\left\{\sum_{j=1}^{(j-1)}\left[\left(\tfrac{F_L L+B_j\varpi}{A_j\varpi}-\tfrac{F_L L+B_{(j+1)}\varpi}{A_{(j+1)}\varpi}\right)L_j-\left(\tfrac{F_L}{2A_j\varpi}-\tfrac{F_L}{2A_{(j+1)}\varpi}\right)L_j^2\right]\right\}x\\&+\sum_{j=1}^{(j-1)}\left[\left(\tfrac{F_L L+B_{(j+1)}\varpi}{2A_{(j+1)}\varpi}-\tfrac{F_L L+B_j\varpi}{2A_j\varpi}\right)L_j^2-\left(\tfrac{F_L}{3A_{(j+1)}\varpi}-\tfrac{F_L}{3A_j\varpi}\right)L_j^3\right].\end{aligned} \tag{21}$$

3.1 Determination of the tip deflection

The tip deflection can be found by substituting $x=L$ in Eqs. 14 and 21.

When $n=1$,

$$\omega_1(L)=\frac{F_L L+B_1\varpi}{2A_1\varpi}L^2-\frac{F_L}{6A_1\varpi}L^3, \tag{22}$$

when $n \geq 2$,

$$\begin{aligned}\omega_n(L)=&\tfrac{F_L L+B_n\varpi}{2A_n\varpi}L^2-\tfrac{F_L}{6A_n\varpi}L^3\\&+\left\{\sum_{j=1}^{(n-1)}\left[\left(\tfrac{F_L L+B_j\varpi}{A_j\varpi}-\tfrac{F_L L+B_{(j+1)}\varpi}{A_{(j+1)}\varpi}\right)L_j-\left(\tfrac{F_L}{2A_j\varpi}-\tfrac{F_L}{2A_{(j+1)}\varpi}\right)L_j^2\right]\right\}L\\&+\sum_{j=1}^{(n-1)}\left[\left(\tfrac{F_L L+B_{(j+1)}\varpi}{2A_{(j+1)}\varpi}-\tfrac{F_L L+B_j\varpi}{2A_j\varpi}\right)L_j^2-\left(\tfrac{F_L}{3A_{(j+1)}\varpi}-\tfrac{F_L}{3A_j\varpi}\right)L_j^3\right].\end{aligned} \tag{23}$$

3.2 Determination of the charge of the piezoelectric layer

The charge appearing on the grounded electrodes of the piezoelectric material in segment j is given by

$$Q_{ij}=\int_0^{\varpi}\int_{L_{(j-1)}}^{L_j} D_{ij}\mathrm{d}x\mathrm{d}y, \tag{24}$$

where D_{ij} is the electric displacement along z-axis inside the piezoelectric material. It is given by the constitutive piezoelectric equation

$$D_{ij}=d_{31ij}T_{xij}+\varepsilon_{ij}E_{ij}, \tag{25}$$

where ε_{ij} is the permittivity of the piezoelectric material.

E_{ij} is equal to zero since both electrodes are grounded. Inserting piezoelectric Eqs. 7 and 25 into 24, the charge can be written as

$$\begin{aligned}Q_{ij}=&\int_0^{\varpi}\int_{L_{(j-1)}}^{L_j} d_{31ij}Y_{ij}(z_{jN}-z)\frac{\partial^2\omega_j}{\partial x^2}\mathrm{d}x\mathrm{d}y\\=&\varpi d_{31ij}Y_{ij}\int_{L_{(j-1)}}^{L_j}(z_{jN}-z)\frac{\partial^2\omega_j}{\partial x^2}\mathrm{d}x\end{aligned} \tag{26}$$

with the Eq. 9, solving 26 leads to

$$Q_{ij} = d_{31ij} Y_{ij} \left(L_j - L_{(j-1)}\right)\left(z_{jN} - z\right) \left(\frac{F_L\left[2L - \left(L_j + L_{(j-1)}\right)\right] + 2B_j\varpi}{2A_j}\right). \quad (27)$$

4 Analysis of the two-layer and two-segment piezoelectric cantilevers

The piezoelectric cantilevers with two-layer and two-segment piezoelectric parts will be analyzed next, based on the generic model of the multimorph beam. The two piezoelectric parts are used to the sensing and actuating element, respectively.

4.1 Two-layer piezoelectric cantilever

Figure 3 shows a schematic sketch of the two-layer piezoelectric cantilever considered in our analysis. Using Eqs. 22 and 27, the tip deflection and the piezoelectric charge are given by

$$\omega_1(L) = \frac{F_L}{3A_1\varpi}L^3 + \frac{B_1}{2A_1}L^2, \quad (28)$$

$$Q_{i1} = d_{31i1} Y_{i1}\left(\frac{F_L L^2}{2A_1} + \frac{B_1 L\varpi}{A_1}\right)\left(z_{N1} - z_{i-1}\right), \quad i = 5, 7. \quad (29)$$

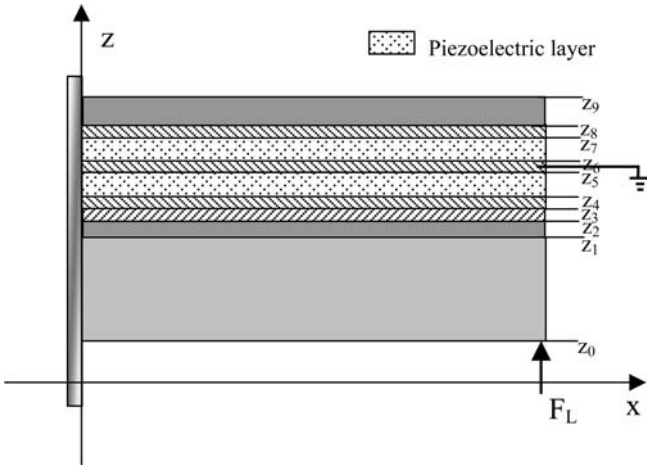

Fig. 3 A multimorph cantilever composed of two piezoelectric layers

For the two-layer piezoelectric cantilever, the two piezoelectric layers can be acted as a force sensor or an actuator. When one piezoelectric layer is acted as an actuator, the other piezoelectric layer will be used as a force sensor. Figure 4 are the plots of the tip deflection ω (L) of the multimorph cantilever and piezoelectric charge Q generated on the sensing element derived in Eqs. 28 and 29 in terms of the silicon substrate thickness and the length of the multimorph cantilever. The characteristics of the multimorph cantilever used for this simulation are given in Table 1. Assuming each layer of the cantilever has the same width that is 200 μm, and the length is in the range of 1,000 μm–2,000 μm. The thickness of the silicon substrate is in the range of 10 μm–20 μm. A voltage of 3 V is applied across the electrodes of the actuating element. The force applied to the tip of the cantilever is 20 μN. Figure 4 shows the

Table 1 Material and geometric parameters of the multimorph cantilevers

	t(μm)	E(GPa)	d_{31}(PC/N)
Layer no 1 (Si)	10∼20	169	
Layer no 2 (SiO_2)	0.5	70	
Layer no 3 (Ti)	0.05	110	
Layer no 4 (Pt)	0.2	145	
Layer no 5 (PZT)	0.25	101	34.1
Layer no 6 (Pt)	0.2	145	
Layer no 7 (PZT)	0.25	101	34.1
Layer no 8 (Pt)	0.2	145	
Layer no 9 (SiO_2)	1	70	

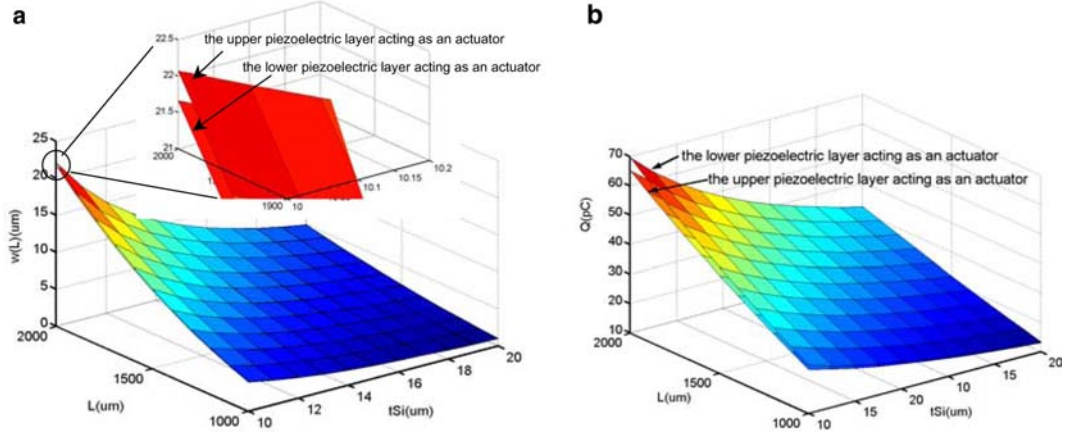

Fig. 4 **a** The tip deflection ω (L) of the multimorph cantilever and **b** piezoelectric charge Q generated on the sensing element, as a function of system geometry

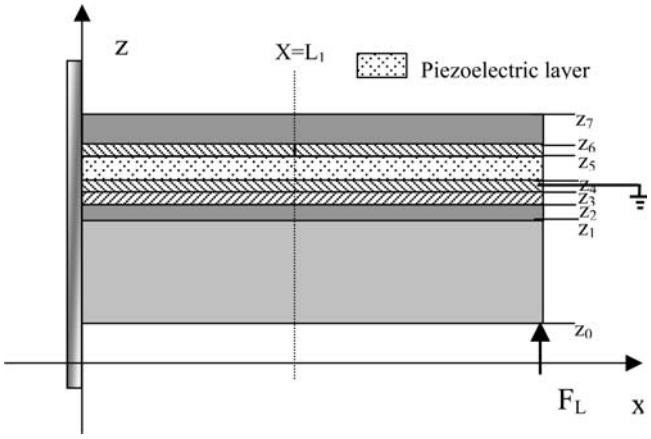

Fig. 5 A multimorph cantilever composed of two piezoelectric segments

comparison between the two cases of the upper and the lower piezoelectric layer acting as an actuator. The tip deflection and the generated piezoelectric charge have slight difference between the two cases. As shown in Fig. 4, when the electric field is applied to upper piezoelectric layer, the two-layer piezoelectric cantilever has a lager tip deflection and a smaller piezoelectric charge than the case that the lower piezoelectric layer is acted as an actuator.

4.2 Two-segment piezoelectric cantilever

Figure 5 shows a schematic sketch of the two-segment piezoelectric cantilever. The tip deflection ω (L) of the cantilever is obtained through replacing n by 2 in Eq. 23.

$$\begin{aligned}\omega_2(L) &= \frac{F_L L+B_2\varpi}{2A_2\varpi}L^2 - \frac{F_L}{6A_2\varpi}L^3 \\ &+\left[\left(\frac{F_L L+B_1\varpi}{A_1\varpi}-\frac{F_L L+B_2\varpi}{A_2\varpi}\right)L_1 - \left(\frac{F_L}{2A_1\varpi}-\frac{F_L}{2A_2\varpi}\right)L_1^2\right]L \\ &+\left[\left(\frac{F_L L+B_2\varpi}{2A_2\varpi}-\frac{F_L L+B_1\varpi}{2A_1\varpi}\right)L_1^2 - \left(\frac{F_L}{3A_2\varpi}-\frac{F_L}{3A_1\varpi}\right)L_1^3\right].\end{aligned} \tag{30}$$

Using Eq. 27, the piezoelectric charge Q generated on the electrodes of the two segments ($j=1,2$) can be written as

$$Q_{51} = d_{3151}Y_{51}L_1\left(\frac{F_L(2L-L_1)+2B_1\varpi}{2A_1}\right)(z_{N1}-z_4), \tag{31}$$

$$Q_{52} = d_{3152}Y_{52}(L-L_1)\left(\frac{F_L(L-L_1)+2B_2\varpi}{2A_2}\right)(z_{N2}-z_4). \tag{32}$$

The material and geometric parameters of the multimorph cantilevers are the same as the two-layer piezoelectric cantilever. Because A_j depends on the elastic and geometric parameters of the cantilever beam, the two segment of the cantilever, A_1 is equal to A_2. There are two working modes for the two-segment piezoelectric multimorph cantilever. When the right segment is acted as an actuator segment, the left piezoelectric segment will be used as a sensor with two grounded electrodes. In this case, B_1 is equal to zero. In the same way, when the left segment is acted as an actuator, B_2 is equal to zero. According to the Eqs. 31 and 32, the piezoelectric charge generated on the sensing element is proportional to the force applied to the tip of the cantilever, and have no relation with the voltage applied to the actuation element. For this two-segment structure, the piezoelectric charge on the sensing element is only produced by the effect of the tip force of the cantilever.

Figure 6 are the plots of the tip deflection of the multimorph cantilever and piezoelectric charge generated on the sensing element in terms of the proportion of the left-segment length (L_1) to the whole length (L) of the cantilever and the thickness of the silicon substrate thickness. When the ratio is equal to 0.293, the two working situations of the two-segment cantilever have the same tip deflection and piezoelectric charge. The result of the comparison between the two cases indicates that when the actuation element produces a larger tip deflection, the sensing element will generate a smaller piezoelectric charge, and vice versa. For the two-segment multimorph cantilever, the relationships of ω (L), Q, versus L, t_{Si} have the same trend with the two-layer multimorph cantilever, as shown in Fig. 7. The proportion of L_1 to L used for this simulation is 0.293.

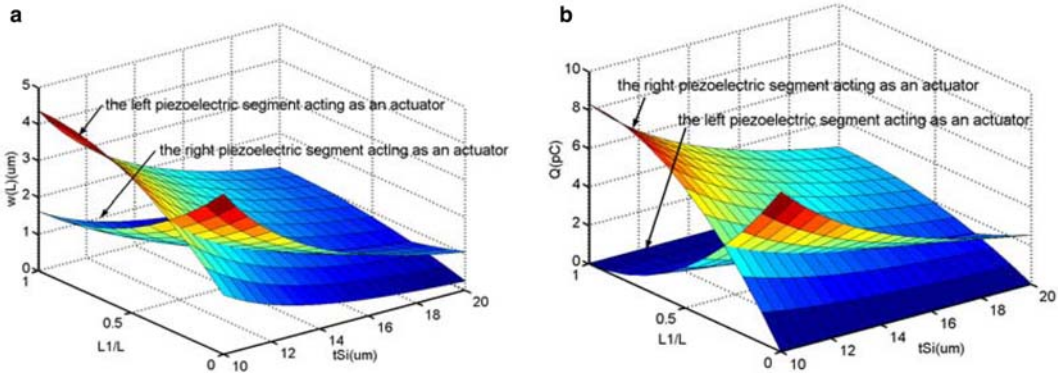

Fig. 6 **a** The tip deflection ω (L) and **b** piezoelectric charge Q generated on the sensing element of the multimorph cantilever as a function of the proportion of the left-segment length (L_1) to the whole (L) length of the cantilever. (Length of the cantilever is 1,000 μm.)

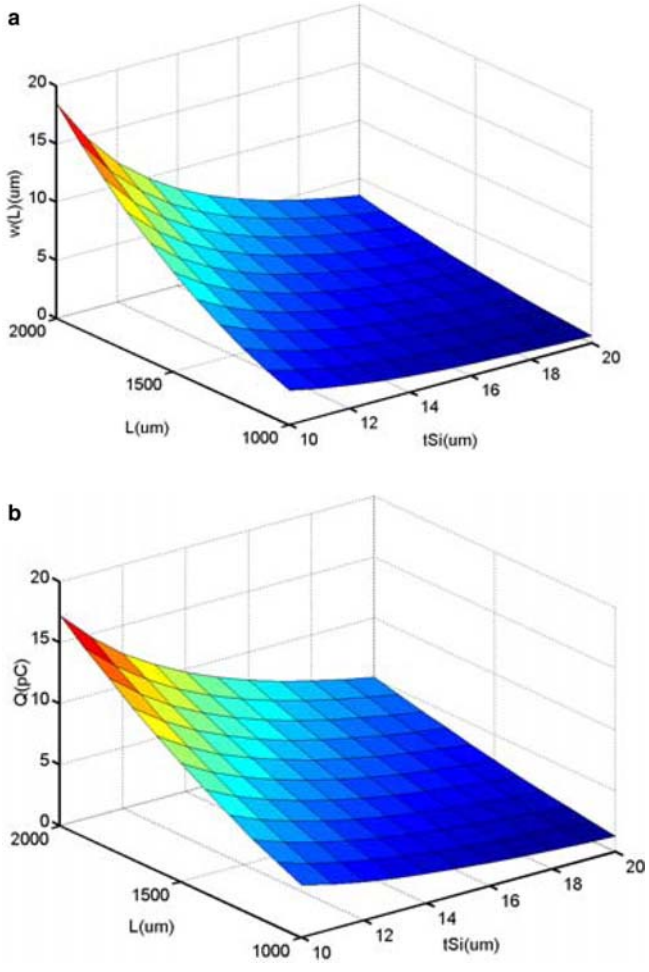

Fig. 7 **a** The tip deflection ω (L) of the multimorph cantilever and **b** piezoelectric charge Q generated on the sensing element as a function of system geometry. ($L1/L = 0.293$)

4.3 Comparison of the two-layer and two-segment piezoelectric cantilevers

The analytical modeling indicates that the tip deflection and piezoelectric charges of two-layer and two-segment cantilevers are proportional to the voltage and tip-force loadings, and they increase as the length increases and the thickness of the silicon substrate decreases. For the two-layer and two-segment piezoelectric cantilevers, there are four working modes, as shown in Fig. 8. To compare the actuating and sensing capabilities of the four different cases, the mulimorph cantilevers are assumed to have the same geometric sizes, the same voltage, and tip-force loadings.

Figure 8 shows the tip deflection ω (L) of the multimorph cantilevers and piezoelectric charge Q generated on the sensing element as a function of L_1/L. The results indicate that the two-layer cantilevers have better actuating and sensing capabilities than the two-segment cantilevers. For the two-layer piezoelectric cantilevers, L_1 is equal to L, so that ω (L) and Q have no relation with the L_1/L. The working situation of the cantilever has less influence to the actuating and sensing capabilities compared with the two-segment cantilever. However, two layers piezoelectric films integrated in the structure make the fabrication of the microcantilever more complex.

5 Conclusion

A theoretical model for piezoelectric multimorph microcantilever with several layers and segments is proposed in the paper. With this model, the sensing and actuating effects of the two-layer and two-segment piezoelectric microcantilever are analyzed. The tip deflection of the cantilever and the piezoelectric charge generated on the sensor element as a function of microcantilever geometry are compared for the different working modes. For the two-layer microcantilevers, ω (L) and Q have slight difference between the two situations when the upper or lower layer is acted as the actuator. For the two working modes of the two-segment microcantilevers, when the left or right segment acts as the actuator, ω (L) and Q have relation with the ratio of the left segment length to the whole length of the

Fig. 8 **a** The tip deflection ω (L) of the multimorph cantilevers (A voltage of 3 V is applied to the actuation element) and **b** piezoelectric charge Q generated on the sensing element (a tip force of 20 μN is applied to the cantilevers) as a function of L_1/L. (The length of the cantilevers is 1,000 μm, and the width of the cantilevers is 200 μm)

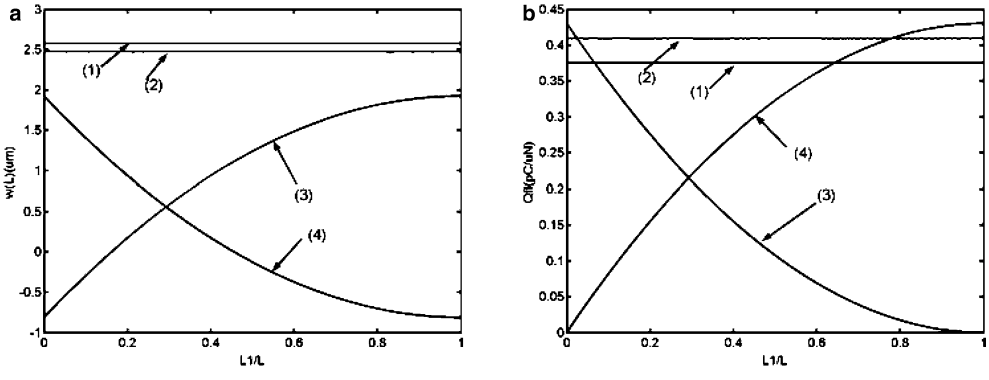

two-layer multimorph cantilever:

(1) the upper piezoelectric layer acting as an actuator

(2) the lower piezoelectric layer acting as an actuator

two-segment multimorph cantilever

(3) the left piezoelectric segment acting as an actuator

(4) the right piezoelectric segment acting as an actuator

cantilever. The comparison between the two working situations indicates that when the actuation element produces a larger tip deflection, the sensing element will generate a smaller piezoelectric charge, and vice versa. For the two types of microcantilevers, the two-layer cantilevers have better actuating and sensing capabilities than the two-segment cantilevers.

Acknowledgments This work is partially supported by the Chinese National Natural Science Fund Project (NSF90207003).

References

Brissaud M, Ledren S, Gonnard P (2003) Modelling of a cantilever non-symmetric piezoelectric bimorph. J Micromech Microeng 13:832–844

Costa Branco PJ, Dente JA (2004) On the electromechanics of a piezoelectric transducer using a bimorph cantilever undergoing asymmetric sensing and actuation. Smart Materials Struct 13:631–642

DeVoe DL, Pisano AP (1997) Modeling and optimal design of piezoelectric cantilever microactuators. J Microelectromech Syst 6(3):266–270

DeVoe DL, Pisano AP (1997) A fully surface-micromachined piezoelectric accelerometer. In: 1997 international conference on solid state sensors and actuators, Chicago, 2:1205–1208

Du Liqun, Kwon Guiryong, Arai Fumihito, Fukuda Toshio, Itoigawa Kouichi, Tukahara Yasunori (2003) Structure design of micro touch sensor array. Sens Actuators A 107:7–13

Elka E, Elata D, Abramovich H (2004) The electromechanical response of multilayered piezoelectric structures. J Microelectromech Syst 13(2):332–341

Garcia E, Lobontiu N (2004) Induced-strain multimorphs for microscale sensory actuation design. Smart Materials Struct 13:725–732

Huang C, Lin YY, Tang TA (2004) Study on the tip-deflection of a piezoelectric bimorph cantilever in the static state. J Micromech Microeng 14:530–534

Itoh T, Suga T (1996) Self-excited force-sensing microcantilevers with piezoelectric thin films for dynamic scanning force microscopy. Sens Actuators A 54:477–481

Kim Hyun Ho, Ju Byeong Kwon, Lee Yun Hi, Lee Si Hyung, Lee Jeon Kook, Kim Soo Won (2001) A noble suspended type thin film resonator (STFR) using the SOI technology. Sens Actuators A 89:255–258

Lee C, Itoh T (1999) Self-excited piezoelectric PZT microcantilevers for dynamic SFM—with inherent sensing and actuating capabilities. Sens Actuators A 72:179–188

Li-Peng Wang, Wolf RA Jr,Yu Wang, Deng KK, Zou L, Davis RJ, Trolier-McKinstry S (2003) Design, fabrication, and measurement of high-sensitivity piezoelectric microelectromechanical systems accelerometers. J Microelectromech Syst 12(4):433–439

Luginbuhl Ph, Racine G-A, De Rooij NF, Lerch Ph, Romanowicz B, Renaud Ph, Brooks KG et al (1996) Piezoelectric cantilever beams actuated by PZT sol-gel thin film. Sens Actuators A 54:530–535

Muralt P (2000) Ferroelectric thin films for micro-sensors and actuators: a review. J Micromech Microeng 10:136–146

de Reus R, Gulløv JO, Scheeper PR (1999) Fabrication and characterization of a piezoelectric accelerometer. J Micromech Microeng 9:123–126

Soderkvist J (1993) Similarities between piezoelectric, thermal and other internal means of exciting vibrations. J Micromech Microeng 3:24–31

Weinberg MS (1996) Working equations for piezoelectric actuators and sensors. J Microelectromech Syst 8(4):529–533

Zhang QQ, Gross SJ, Tadigadapa S, Jackson TN, Djuth FT, Trolier-McKinstry S (2003) Lead zirconate titanate films for d_{33} mode cantilever actuators. Sens Actuators A 105:91–97

Zurn S, Hsieh M, Smith G, Markus D, Zang M, Hughes G, Nam Y, Arik M, Polla D (2001) Fabrication and structural characterization of a resonant frequency PZT microcantilever. Smart Materials Struct 10:252–263